NIH Public Access
Author Manuscript
*J Cell Physiol*. Author manuscript; available in PMC 2014 November 01.

Published in final edited form as:
*J Cell Physiol*. 2013 November ; 228(11): 2127–2138. doi:10.1002/jcp.24375.

# Polycyclic Aromatic Hydrocarbons—Induced ROS Accumulation Enhances Mutagenic Potential of T-Antigen From Human Polyomavirus JC

**ANNA WILK**[1,2], **PIOTR WALIGÓ RSKI**[1,2], **ADAM LASSAK**[1,2], **HIMANSHU VASHISTHA**[1,3], **DAVID LIRETTE**[4], **DAVID TATE**[2], **ARNOLD H. ZEA**[2], **SHAHRIAR KOOCHEKPOUR**[5], **PAULO RODRIGUEZ**[2], **LEONARD G. MEGGS**[3], **JOHN J. ESTRADA**[2], **AUGUSTO OCHOA**[2], and **KRZYSZTOF REISS**[1,2,*]

[1]Neurological Cancer Research at Stanley S Scott Cancer Center, New Orleans, Louisiana

[2]Stanley S. Scott Cancer Center, New Orleans, Louisiana

[3]Department of Nephrology, Ochsner Medical Center, New Orleans, Louisiana

[4]Department of Medicine, School of Public Health, LSU Health Sciences Center, New Orleans, Louisiana

[5]Department of Cancer Genetics and Urology, Roswell Park Cancer Institute, Buffalo, New York

## Abstract

Polycyclic aromatic hydrocarbons (PAHs) are the products of incomplete combustion of organic materials, which are present in cigarette smoke, deep-fried food, and in natural crude oil. Since PAH-metabolites form DNA adducts and cause oxidative DNA damage, we asked if these environmental carcinogens could affect transforming potential of the human Polyomavirus JC oncoprotein, T-antigen (JCV T-antigen). We extracted DMSO soluble PAHs from Deepwater Horizon oil spill in the Gulf of Mexico (oil-PAHs), and detected several carcinogenic PAHs. The oil-PAHs were tested in exponentially growing cultures of normal mouse fibroblasts (R508), and in R508 stably expressing JCV T-antigen (R508/T). The oil-PAHs were cytotoxic only at relatively high doses (1:50–1:100 dilution), and at 1:500 dilution the growth and cell survival rates were practically unaffected. This non-toxic dose triggered however, a significant accumulation of reactive oxygen species (ROS), caused oxidative DNA damage and the formation of DNA double strand breaks (DSBs). Although oil-PAHs induced similar levels of DNA damage in R508 and R508/T cells, only T-antigen expressing cells demonstrated inhibition of high fidelity DNA repair by homologous recombination (HRR). In contrast, low-fidelity repair by non-homologous end joining (NHEJ) was unaffected. This potential mutagenic shift between DNA repair mechanisms was accompanied by a significant increase in clonal growth of R508/T cells chronically exposed to low doses of the oil-PAHs. Our results indicate for the first time carcinogenic synergy in which oil-PAHs trigger oxidative DNA damage and JCV T-antigen compromises DNA repair fidelity.

© 2013 Wiley Periodicals, Inc.

[*]Correspondence to: Krzysztof Reiss, Department of Medicine, LSU Health Sciences Center, Neurological Cancer Research, Stanley S. Scott Cancer Center, 533 Bolivar St. Room 525, New Orleans, LA 70112. kreiss@lsuhsc.edu.
Anna Wilk and Piotr Waligórski contributed equally to this work.

NIH-PA Author Manuscript
NIH-PA Author Manuscript
NIH-PA Author Manuscript

NIH-PA Author Manuscript

NIH-PA Author Manuscript

NIH-PA Author Manuscript

Human neurotropic polyomavirus JC (JCV) infects nearly 80% of human population. Primary infections happen during childhood, are asymptomatic in healthy individuals, and the virus is suspected of remaining latent in kidneys and possibly in the brain (Major et al., 1992; Reiss and Khalili, 2003; Rollison et al., 2003; Reiss et al., 2010). During severe immunodeficiency, JCV can reactivate in oligodendrocytes causing progressive multifocal leucoencephalopathy (PML)—a devastating disease often affecting patients with AIDS (Berger and Concha, 1995; Matsiota-Bernard et al., 1997). In immunocompetent individuals, expression of viral proteins, including transforming antigens (large and small T-antigens), can happen in the absence of viral replication (Khalili et al., 1999; Krynska et al., 1999; Del Valle et al., 2001a; Reiss and Khalili, 2003). These viral proteins are known to dysregulate cell control mechanisms responsible for DNA replication, cell survival, and DNA repair (Krynska et al., 2000; Trojanek et al., 2006a,b). In addition, polyomavirus T-antigens transform cells in vitro; are tumorigenic in experimental animals; and several reports demonstrated their presence in clinical samples from human tumors (Del Valle et al., 2001a, 2002a; Reiss and Khalili, 2003; Reiss et al., 2010). In spite of these findings and considering very high prevalence of JCV in human population, the number of human tumors in which T-antigens have been detected is relatively small. This may suggest that other environmental and/or genetic predispositions could be required to initiate and/or enhance T-antigen-induced malignant transformation in humans.

Polycyclic Aromatic Hydrocarbons (PAHs) are present in cigarette smoke, deep-fried food, and are abundant in natural crude oil (Al-Hashem et al., 2007; Goldstein et al., 2011; Dickey, 2012; Rotkin-Ellman et al., 2012). Large-scale oil spills such as the Deepwater Horizon (DWH) oil spill in the Gulf of Mexico in 2010, contribute to the overall increase in PAHs concentration in water, soil, and air. Although chronic effects of low doses of PAHs on human health are not well defined, several PAHs are classified as potent carcinogens, which can form covalent DNA adducts and cause oxidative DNA damage (Seike et al., 2003; Xue and Warshawsky, 2005; Ji et al., 2010; Liu et al., 2010). These primary DNA lesions may result in the accumulation of random mutations when cellular mechanisms responsible for DNA repair fidelity are compromised. In this regard, our previous studies demonstrate that JCV large T-antigen (JCV T-antigen), in addition to its well documented role in reactivating cell proliferation (Brodsky and Pipas, 1998; Sullivan et al., 2000), can compromise DNA repair fidelity by inhibiting homologous recombination directed DNA repair (HRR) (Reiss et al., 2006; Trojanek et al., 2006a,b; Reiss et al., 2012).

In the present study we ask if PAHs extracted from the natural crude oil affect transforming potential of the JCV T-antigen. We demonstrate that DMSO soluble PAHs obtained from the 2010 DWH oil spill (oil-PAHs) contain a mixture of at least five carcinogenic PAHs. Chronic cell exposure to the oil-PAHs resulted in excessive ROS accumulation, which resulted in oxidative DNA damage and triggered DNA double strand breaks (DSBs) in cells replicating DNA. Importantly, ROS scavengers, *N*-acetyl cysteine (NAC) and Trolox, attenuated both ROS accumulation and DNA damage. In addition, JCV T-antigen positive cells exposed to low doses of the oil-PAHs, demonstrated a shift from HRR to less faithful NHEJ, which correlated with a significant increase in their clonogenic growth. Considering that oil-PAH-induced oxidative DNA damage potentiates carcinogenic effects of JC virus,

NIH-PA Author Manuscript

NIH-PA Author Manuscript

NIH-PA Author Manuscript

and that polyomaviruses are ubiquitous in humans, vaccination against the virus and the use of antioxidants should be considered at least for populations at high risk of long-term exposure.

## Materials and Methods

### PAHs samples

Natural crude oil was obtained from 2010 Deep Water Horizon (DWH) oil spill in the Gulf of Mexico. The sample was collected from BP-MS Canyon 252 (Discover Enterprise sample #011 obtained in May 20, 2010 at 11:15 am) and transported to the lab in air- and light-tight bottle at 4°C. For DMSO extraction of aromatic components, crude oil was diluted in DMSO (1:100, v/v). The obtained mixture was stirred at room temperature for 4 h with occasional gentle mixing every 30 min. Next, the surface oil fraction was removed and the oil-free solution was diluted 10 times in double distillated water. After mixing, the solution was filtered and frozen at −20°C in 5 ml aliquots (oil-PAHs).

### High performance liquid chromatography (HPLC)

The PAH-DMSO extracts were analyzed by HPLC (Dionex Ultimate 3000; Sunnyvale, CA) with a photodiode array UV detector. Chromatographic separation was achieved using a 150-by 4.6-mm (inner diameter) $C_{18}$ reverse-phase column (particle size, 3 μm; ACCLAIM 120 C-18). The column was equilibrated at flow rate 0.5 ml/min with mobile-phase consisting of 60% water and 40% acetonitrile followed by a linear gradient to 100% acetonitrile. Detection was monitored with UV at an absorbance of 254 nm. The obtained peaks of oil-PAHs were identified and quantified by comparing them with corresponding retention times, spectra, and concentrations of the standard PAHs (Fig. 1C).

### Cell culture

To analyze potential mutagenic interaction between oil-PAHs and viral oncoprotein, JCV T-antigen, we used JCV T-antigen positive (R508/T) and negative (R508) mouse embryo fibroblasts, as well as R508 cells stably expressing DRGFP reporter (R508/DRGFP)—to evaluate HRR. All R508 cells, including R508/T, although are immortalized, do not grow well in semi-solid culture conditions (soft agar; Del Valle et al., 2002b). These cells were generated and characterized in our previous studies (Del Valle et al., 2002b) and are well suited to evaluate changes in cell proliferation, survival, transformation and DNA repair (Trojanek et al., 2003). The cells are routinely cultured in DMEM (GIBCO BRL, Grand Island, NY) supplemented with 10% FBS (Sigma, St. Louis, MO), 50 U/ml penicillin, 50 ng/ml streptomycin, and 250 μg/ml hygromycin at 37° C in a 5% $CO_2$ atmosphere. In some experiments oil-PAHs were added to culture media in dilutions ranging from 1:50 to 1:1,000 in the presence or absence of ROS scavengers, *N*-acetyl cysteine (NAC, 1 mM) and Trolox (100 μM).

### ROS measurements

Accumulation of reactive oxygen species (ROS) was evaluated following cell exposure to oil-PAHs for 72 h. The oil-PAHs were tested in two dilutions (1:100 and 1:500 in DMEM + 10% FBS). The cells were also treated with the mixture of PAHs (mix-PAHs) prepared

NIH-PA Author Manuscript

NIH-PA Author Manuscript

NIH-PA Author Manuscript

accordingly to the content of PAHs detected in DMSO fraction from DWH natural crude oil (Fig. 1). Intracellular ROS was measured in Synergy 2 micro-plate reader by utilizing 2′,7′-Dichlorofluorescin diacetate (H2DCFDA), which is cell permeable, non-fluorescent compound. When H2DCFDA is oxidized it changes into the green fluorescent dye, fluorescein. After exposure to oil-PAHs, for 72 h, the cells were washed with PBS and incubated in 1 ml of phenol red-free culture medium containing 10 μl of H2DCFDA (stock solution: 50 μg H2DCFDA in 86.5 μl DMSO) in the dark at 37°C for 30 min. The cells were washed with PBS again, and 250 ul phenol red-free culture media (without H2DCFDA) was placed into each well. The fluorescence was measured (excitation/494 nm; emission/521 nm) every 5 min for 30 min. ROS accumulation was expressed as fluorescence intensity unit per time and cell number. In some experiments, the cells preloaded with H2DCFDA were analyzed using flow cytometry (GUAVA easyCyte 8HT).

### Cell cycle distribution and cell survival

Briefly, the aliquots of $1 \times 10^6$ cells/ml were fixed in 70% ethanol at −20°C, overnight. The cells were centrifuged at 1,600 rpm and the resulting pellets suspended in 1 ml of freshly prepared Propidium Iodide/RNaseA solution. Cell cycle distribution was evaluated in GUAVA easyCyte 8HT using GuavaSoft 1.1. Cell death was evaluated by the assay based on cell membrane integrity using ViaCount reagents (Millipore, Billerica, MA) and Guava/ViaCount software was used for data analysis.

### Neutral comet assay

Neutral comet assay was utilized to detect DNA strand breaks in exponentially growing JCV T-antigen positive and negative R508 cells in the presence and absence of oil-PAHs. The cells treated with H2O2 (oxidative DNA damage) or neocarzinostatin (NCS; Sigma) were used as positive controls for secondary and primary DNA double strand breaks (DSBs), respectively. The cells were subjected to single cell electrophoresis in neutral conditions (Collins et al., 2008) and processed by utilizing SYBR green based kit from Trevigen and Automated Comet Assay System from Loats Associates, Inc. The tail moment was calculated from 100 cells collected per single measurement in triplicate using Automated Comet Assay System software (Loats Associates, Inc., Westminster, MD).

### Immunofluorescence

All cells were cultured on glass culture slides (BD Falcon, Franklin Lakes, NJ). For immunostaining the cells were fixed and permeablized with the buffer containing 0.02% Triton X-100 and 4% formaldehyde in PBS. 8-hydroxy-2-deoxyguanosine (8-oxo-dG) was detected by mouse anti-8-oxo-dG monoclonal antibody (Millipore) followed by AlexaFluor-conjugated anti-mouse secondary antibody (Invitrogen, Carlsbad, CA). Phosphorylated form of histone H2AX (S139; γH2AX) was detected by rabbit polyclonal antibody (Millipore), and rhodamine-conjugated goat anti-rabbit secondary antibody (Molecular Probes, Eugen, OR). The images were visualized with the Nikon Eclipse E400 upright fluorescence microscope equipped with EXI aqua camera (Qimaging, Surrey, BC), motorized *Z*-axis, and SlideBook5 acquisition/deconvolution software (Intelligent Imaging Innovations, Inc., Denver, CO). Quantification of 8-oxo-dG and γH2AX labeling was performed by utilizing

NIH-PA Author Manuscript

NIH-PA Author Manuscript

NIH-PA Author Manuscript

Mask analysis included in SlideBook5 software according to manufacturer recommendation (Intelligent Imaging Innovations, Inc.).

### Oxidative DNA damage

8-oxo-dG immunolabeling was performed on formaldehyde-fixed monolayer cultures of R508 and R508/T cells treated with oil-PAHs (1:500 dilution) for 14 days. The content of 8-oxo-dG in urine was detected by ELISA kit provided by ACE, measured by Synergy-2 microplate-reader (BioTek, Winooski, VT), and calculated by the Gen5 software. Parallel urine samples were analyzed for urinary creatinine (ELISA kit; ExoCell, Inc., Philadelphia, PA) to normalize 8-oxo-dG content. The urine samples were obtained from SV129 mice (3 months old) fed once a day with vehicle (50 μl of DMSO) or with oil-PAHs (50 μl of undiluted DMSO-PAHs fraction) administered by oral gavage. Every seventh day, mice were transferred to metabolic cages (TechniPlast, Buguhhiate, VA) and urine samples were collected for 24 h. The oil-PAHs dilution was calculated per body weight of the animal, and was approximated as 1:800.

### Lipid peroxidatoion

Accumulation of Malondialdehyde (MAD) as a natural product of lipid peroxidation was evaluated using MDA Assay Kit according to the manufacturer recommendations (BioVision, Milpitas, CA) in cells exposed to the oil-PAHs (1:100) for 72 h.

### DNA repair of double strand breaks (DSBs)

To evaluate NHEJ, we have used previously described cell-free assay with some modifications (Trojanek et al., 2006b). NHEJ reaction mix contained: 50 μg of nuclear lysate, 1 mM ATP, 0.25 mM deoxynucleoside triphosphates, 25 mM Tris acetate (pH 7.5), 100 mM potassium acetate, 10 mM magnesium acetate, and 1 mM dithiothreitol. After 5 min of preincubation at 37°C, it was supplemented with the substrate [500 ng of *Xho*I-linearized pBluescript KS(+)]. The reaction mixture was incubated for 1 h at 37°C to ligate the plasmid and was treated with proteinase K (1 μg per reaction at 62°C for 60 min) to digest DNA-bound proteins. NHEJ products were resolved in a 0.6% agarose gel containing ethidium bromide (0.5 μg/ml).

HRR was assessed using the reporter plasmid pDR-GFP (Pierce et al., 1999) generously provided by M. Jasin (Sloan-Kettering Cancer Center). A stable clone of R508 cells expressing the construct (R508/DRGFP) was previously characterized (Trojanek et al., 2003). Briefly, the pDR-GFP reporter contains inactive green fluorescent protein (GFP) gene (SceGFP) as a recombination reporter and a fragment of the GFP gene as a donor for homologous repair. The SceGFP cassette has an inactivating insertion, which consists of two stop codons and a restriction site for the rare-cutting endonuclease I-*Sce*I. When I-*Sce*I is expressed in DR-GFP-expressing clones, it inflicts DSBs within the SceGFP fragment, providing a signal for homologous recombination and the reconstruction of functional GFP (Pierce et al., 1999).

NIH-PA Author Manuscript

NIH-PA Author Manuscript

NIH-PA Author Manuscript

### Clonogenic growth

Exponentially growing R508 and R508/T cells (10% FBS) were either treated with DMSO (control) or with oil-PAHs 1:500 for 4 weeks. Next the cells were washed with fresh serum-free medium, trypsinized and transferred to 35 mm culture dishes at clonal-density ($1 \times 10^3$ cells/35 mm dish). Clonogenic growth was evaluated after additional 2 weeks of a continuous cell growth in media containing 10% FBS + DMSO or 10% FBS + PAHs 1:500. The resulting clones were fixed and stained with 0.25% cristal violet in methanol.

### Statistical analysis

The data were analyzed with homoscedastic Student's *t*-test. The differences between the control and experimental groups were considered significant and marked with asterisk ($^*$) for *P* values lower than 0.05.

## Results

### PAH content in DMSO crude oil fraction

We have characterized DMSO soluble PAHs from 2010 Deepwater Horizon (DWH) oil spill in the Gulf of Mexico (oil-PAHs). Figure 1 demonstrates results from HPLC analysis of this fraction (Parts A and B). The HPLC parameters were set for detection and quantification of oil-PAHs using a mixture of 13 standard PAHs (Part C). The peaks, which demonstrated identical retention times and identical spectral profiles (excitation, emission, and absorption maxima) in comparison with standard PAHs, were selected. This approach allowed identification and quantification of the following PAHs: fluoranthene (26.6 μg/ml), pyrene (11.1 μg/ml), benzo-α-pyrene (8.1 μg/ml), phenanthrene (3.9 μg/ml), and chrysene (3.8 μg/ml), which according to NCI Chemical Carcinogen Reference Standards Repository, Catalog 2010, are carcinogenic. We have tested the obtained oil-PAHs in cell culture and in mice using subsequent dilutions: 1:50, 1:100, 1:500, 1:800, and 1:1,000. The last column in Figure 1B demonstrates final concentrations of the five oil-PAHs at 1:500 dilution. Some experiments were repeated with purified PAHs (Fig. 1C, highlighted yellow), which were pre-mixed and diluted in DMSO according to the PAH-content found in DWH crude oil DMSO extract, and are labeled as mix-PAHs.

### Cytostatic and cytotoxic effects of oil-PAHs

We evaluated first how different dilutions of oil-PAHs affect cell proliferation and cell survival. This was critically important in view of a possible contribution of PAHs in supporting mutagenic action of JCV T-antigen. If PAHs could indeed potentiate malignant transformation by JCV T-antigen, affected cells should be able to proliferate during the treatment. Only in such condition acquired mutations could be passed to the next generation contributing to the selection of clones with growth and/or survival advantage. The results in Figure 2 show cell cycle analysis (Part A), cell survival (Part B), and cell growth (Part C) of R508 and R508/T cells exposed to the oil-PAHs. Interestingly, cell cycle distribution (Part A) and cell growth (Part C) were practically the same in DMSO control cultures and in cultures exposed to the oil-PAHs at 1:1,000 and 1:500 dilutions. Only at higher doses (oil-PAHs diluted 1:50 and 1:100), both R508 and R508/T were characterized by G1 arrest. In

NIH-PA Author Manuscript

NIH-PA Author Manuscript

NIH-PA Author Manuscript

respect to cell viability, we did not observe any measurable cell death at 1:1,000 and 1:500 dilutions. At 1:100, oil-PAHs induced cell death in 12% and 7% of R508 and R508/T, respectively (Part B), which was accompanied by a proportional decline in the growth rate (Part C). Finally, at 1:50 dilution oil-PAHs were highly cytotoxic to both cell lines, and cell death levels were comparable to those detected in the presence of DNA-damaging agent, cisplatin (1 μg/ml). These results allowed us to select 1:500 dilution in which both R508 and R508/T cells were able to proliferate for many generations.

### PAH-induced ROS accumulation and oxidative DNA damage

In spite of the low cytotoxicity, oil-PAHs at 1:500 dilution triggered accumulation of the reactive oxygen species (ROS; Fig. 3A,B). The kinetics of ROS accumulation were evaluated in living cells pre-loaded with ROS sensitive fluorescent dye, 2′,7′-dichlorofluorescin-diacetate (H2DCFDA). The results in Figure 3A show that in comparison to DMSO-treated controls, R508 cells treated with oil-PAHs, 1:500 and 1:100 dilution, demonstrated over fivefold and sevenfold increase in ROS-dependent fluorescence, respectively. This PAH-induced ROS accumulation was effectively quenched in the presence of ROS scavenger, NAC. We have confirmed these findings by flow cytometry-based measurement of ROS (Fig. 3B). In addition, we have compared ROS levels in R508 cells, which were either exposed to the oil-PAHs or to the individual PAHs premixed in DMSO in the proportion corresponding to the content of PAHs in the natural crude oil (Fig. 1). The results in Figure 3B demonstrated sixfold and threefold increase in ROS accumulation when oil-PAHs (1:500), or the mixture of synthetic PAHs (mix-PAHs; 1:500) were used, respectively. Although both oil-PAHs and mix-PAHs triggered ROS accumulation, oil-PAHs are significantly more potent (Fig. 3B; compare second and fourth part in the first row). This discrepancy could indicate that other components extracted from the natural crude oil also contribute to the observed ROS accumulation. We have also evaluated effects of the oil-PAHs on ROS accumulation in cells expressing JCV T-antigen. In comparison to R508, R508/T cells demonstrated significantly higher accumulation of ROS in both control conditions (DMSO) and following PAH treatment (Fig. 3B; compare date in the first [R508] and second [R508/T] row). Also here ROS scavengers, NAC, and less effectively, Trolox, attenuated PAH-induced ROS accumulation.

This intracellular ROS accumulation observed in the presence of the oil-PAHs was accompanied by elevated oxidative DNA damage, detected here by 8-Oxo-2′-deoxyguanosine (8-oxo-dG) immunolabeling. 8-oxo-dG, is a stable product of DNA repair, which can be detected in cytoplasm, extracellular matrix, blood, saliva, and urine (Loft et al., 1999; Poulsen et al., 1999; Park et al., 2005). The results in Figure 3C show a strong cytosolic immunolabeling with anti-8-oxo-dG antibody (green fluorescence) following 14 days of a continuous cell exposure to oil-PAHs (1:500). Surprisingly, detected oxidative DNA damage, both basal (DMSO) and PAH-induced was similar in R508 and R508/T cells, despite of a significantly higher level of ROS in T-antigen expressing cells (compare Fig. 3B,C).

At this point we assumed that PAH-induced ROS is generated mostly inside the cell. This is because intracellular aldo-keto reductase activity is necessary to convert PAH-metabolites to

NIH-PA Author Manuscript

NIH-PA Author Manuscript

NIH-PA Author Manuscript

PAH-o-quinones, which are strong electron acceptors, and can cause extensive oxidative damage (Burczynski and Penning, 2000; Park et al., 2008). To determine if oil-PAHs could also cause membrane lipids peroxidatidation, we evaluated this parameter using Lipid Peroxidation (MDA) Assay Kit (BioVision). The results in Figure 3D demonstrate detectable levels of lipid peroxidation in control (DMSO treated cells), and consistently higher values in samples treated with oil-PAHs at 1:500 ($P = 0.0215$) and 1:100 ($P = 0.0129$) dilutions.

Since effects of the oil-PAHs on DNA oxidation were much more pronounced in comparision to lipids peroxidation, we tested this parameter in mice. Results in Figure 3E demonstrate almost fourfold increase in urinary 8-oxo-dG in mice fed with the oil-PAHs for a period of 4 weeks (oil-PAHs 1:800 dilution/body weight), further supporting a significant DNA damaging effect of this environmental contaminants in living organisms.

### Effects of oil-PAHs on DNA double strand breaks (DSBs)

We asked next if oil-PAHs could contribute to the formation of DNA strand breaks in cells replicating DNA. The results in Figure 4A demonstrate nuclear labeling for DSBs marker, phosphorylated histone H2AX (γH2AX). The positive nuclear foci (green fluorescence) were formed at much higher level in cells exposed to oil-PAHs. In comparison with vehicle-treated cells (DMSO), a significant 3-fold and 2.5-fold increase in γH2AX nuclear foci (γH2AX/DAPI co-localization per nucleus) was observed in R508 and R508/T, respectively (Fig. 4B). In addition to γH2AX evaluation, we have tested DSBs formation by neutral comet assay (Fig. 4C). In comparison to DMSO-treated controls, oil-PAH-treated R508 cells demonstrated 4.3-fold increase in comet tail moment; and in R508/T cells oil-PAHs induced 4.6-fold increase. Importantly, PAH-induced DSBs were effectively attenuated by ROS scavengers NAC and Trolox, indicating that ROS accumulation contributes to this process. We have also observed an increase in DSBs in cells treated with the mixture of synthetic PAHs (mix-PAHs; Fig. 4C). In this instance mix-PAHs were again less potent than oil-PAHs, which indicate that other components extracted from the natural crude oil, like for instance heavy metals (Jomova and Valko, 2011), could contribute to the observed DNA damage.

### Effects of oil-PAHs on homologous recombination directed DNA repair (HRR) and non-homologous end joining (NHEJ)

We have previously reported that JCV T-antigen inhibits HRR with no apparent effect on NHEJ (Trojanek et al., 2006a,b). Since our data demonstrate that the non-toxic levels of oil-PAHs induce DSBs in cells replicating DNA, we asked if oil-PAHs could also affect DNA repair. To evaluate HRR, we used R508 cells stably expressing DR-GFP reporter vector (Trojanek et al., 2006a). The results in Figure 5A demonstrate flow cytometry-based evaluation of HRR, which demonstrates that R508/DRGFP cells exposed to oil-PAHs (1:500) utilize significantly less HRR in comparison to DMSO-treated control cells (24% decrease; $P = 0.0023$). To analyze JCV T-antigen contribution in this process, we have transfected R508/DRGFP cells with pCDNA3/JCV-T/Zeo expression vector (Trojanek et al., 2006a) and the resulting cells were exposed either to oil-PAHs (1:500) or to DMSO for 96 h. The results in Figure 5B demonstrate immunofluorescent detection of JCV T-antigen

NIH-PA Author Manuscript

NIH-PA Author Manuscript

NIH-PA Author Manuscript

(red fluorescence) and cytofluorescent detection of reconstituted DR-GFP reporter (green fluorescence) in which most of the cells expressing T-antigen are negative for DNA repair by HRR (lack of co-expression of green and red fluorescence). Two cells indicated by the arrow represent a rare example of HRR-mediated DNA repair in the presence of JCV T-antigen. Quantitatively, only 5.6 ± 1.25% of T-antigen expressing cells were able to utilize HRR to repair I-Sce-1 induced DSBs (co-expression of green and red fluorescence), which was further reduce to 2.4 ± 0.9% in the presence of oil-PAHs. This 57.2% decrease was statistically significant (Fig. 5C). In the absence of T-antigen almost 11% of the cells utilize HRR and oil-PAHs decreased this value to 9%; and in difference to the results in Figure 5A, this 18% decrease in HRR was not significant.

In respect to NHEJ, oil-PAHs used at 1:500-dilution did not affect this DNA repair process, however, some inhibition was detected at 1:100-dilution (Fig. 6A). We have previously reported that JCV T-antigen does not affect NHEJ (Trojanek et al., 2006a), which supports the idea that T-antigen expressing cells growing in the presence of oil-PAHs, could still utilize mutagenic NHEJ when HRR is severely impaired. In such condition, spontaneous mutations may accumulate increasing probability of malignant transformation.

To test this assumption, we have compared clonal growth of R508 and R508/T cells chronically exposed to oil-PAHs (1:500). The results in Figure 6C demonstrate that clonogenic potential of R508 cells is low (18 ± 5 clones were formed from $1 \times 10^3$ cells); and the cells exposed to oil-PAHs, for 6 weeks, formed 24.2 ± 5 clones. However, this 26% increase did not reach statistical significance ($P = 0.137$). In comparison, untreated R508/T cells formed 91 ± 10 clones, and the oil-PAH treatment resulted in the formation of an average of 166.6 ± 17 clones, and this 82% increase was highly significant ($P = 0.000033$).

## Discussion

The results of this study demonstrate that DMSO extract of the natural crude oil contains at least five carcinogenic PAHs (oil-PAHs). When tested in exponentially growing R508 mouse embryo fibroblasts, and in R508 cells stably expressing viral oncoprotien, JCV T-antigen (R508/T), oil-PAHs were cytotoxic only at relatively high dose (oil-PAHs diluted 1:50), and at 1:500 dilution the exposed cells were able to proliferate for many generations. However, at this non-toxic level oil-PAHs triggered intracellular ROS accumulation, and caused oxidative DNA damage, and DNA double strand breaks (DSBs). Although oil-PAHs induced similar DNA damage in R508 and R508/T cells, the impairment of high fidelity HRR was much more evident in cells expressing JCV T-antigen. In contrast, low-fidelity NHEJ was practically unaffected. Importantly, this potentially mutagenic shift from HRR to NHEJ was accompanied by a significant increase in clonal growth of R508/T cells chronically exposed to the oil-PAHs.

Multiple reports including our own studies indicate that JC virus and PAHs are independent risk factors for tumor development. For example, the viral oncoprotein, JCV T-antigen, is transforming in vitro (Sullivan et al., 2000; Del Valle et al., 2002b), is tumorigenic in experimental animals (Del Valle et al., 2001b), and has been detected in a variety of tumor clinical samples including lung (Abdel-Aziz et al., 2007) and colon cancer (Del Valle and

NIH-PA Author Manuscript

NIH-PA Author Manuscript

NIH-PA Author Manuscript

Khalili, 2010), and CNS malignances (Khalili et al., 1999; Del Valle et al., 2001a,b). In respect to PAHs, these common environmental contaminants have been linked to skin, bladder, and lung cancer (Boffetta et al., 1997; Gammon and Santella, 2008; Sankpal et al., 2012). An elevated risk for brain tumors has been documented among petroleum refinery workers (Alexander et al., 1980; Demers et al., 1991; Carozza et al., 2000). In addition, one of the best-studied PAHs, benzo(α)pyrene, has been shown to inflict extensive DNA damage in different tissues (Demers et al., 1991).

Genotoxic effects of lipophilic PAHs require metabolic processing towards more hydrophilic intermediate metabolites (Stowers and Anderson, 1985). In particular, PAHs can be metabolized to diol-epoxide derivatives by cytochrome P450-dependent monooxygenase and epoxide hydrolase, which are capable of forming covalent DNA adducts (Stowers and Anderson, 1985; Curfs et al., 2003). In addition, aldo-keto reductase can further convert PAH-metabolites to PAH-o-quinones, which are strong electron acceptors, and can cause extensive oxidative damage (Burczynski and Penning, 2000; Park et al., 2008). Importantly, both oxidative DNA damage and DNA adducts can initiate DNA double strand breaks (DSBs) when left unrepaired in cells replicating DNA (Hoeijmakers, 2001; Nakanishi et al., 2011). Indeed, our results in Figure 4 confirm such a possibility in our experimental setting. In addition, PAH-induced DSBs diminished significantly in the presence of ROS scavengers, NAC and Trolox (Fig. 4), suggesting that oxidative DNA damage may indeed contribute to this potentially mutagenic process.

DSBs activate DNA-dependent kinases such as DNA PK, ATM, and ATR (Hoeijmakers, 2001; Wilk et al., 2012), which phosphorylate histone H2AX at the sites surrounding DSBs, leading to the recruitment of two major DSBs repair mechanisms: HRR, which is considered faithful; and less faithful NHEJ (Reiss et al., 2006). It has been also proposed that a proper balance between HRR and NHEJ may play a role in the maintenance of genomic integrity (Hoeijmakers, 2001; Reiss et al., 2006; Kass and Jasin, 2010). However, if HRR is impaired and unrepaired DSBs are processed by NHEJ, it may lead to the accumulation of random mutations especially in cells replicating DNA. In this respect, our previous studies demonstrated that JCV T-antigen, in addition to its well-documented role in triggering abnormal cell proliferation, inhibited HRR and compromised DNA repair fidelity (Reiss et al., 2006; Trojanek et al., 2006a,b). Therefore, mutagenic conditions may occur if the cells attempt to repair PAH-inflicted DSBs in the presence of JCV T-antigen. Although accumulation of random mutations does not necessary mean malignant transformation, our results in Figure 6C demonstrate a significant increase in clonal growth of T-antigen expressing cells chronically exposed to oil-PAHs, which could provide the first step in the process of malignant transformation. Since large-scale oil spills increase overall PAH concentrations in the air, soil, and water, the long-term health impact could be significant, especially in the populations from the affected coastal areas. It should be emphasized, however, that despite of this apparent in vitro correlation between expression of JCV T-antigen, cell exposure to oil-PAHs, and elevated clonogenicity, it is difficult to approximate how the oil-PAH dilutions we are using in this study translate to the real uptake and accumulation of these carcinogens in the human body.

NIH-PA Author Manuscript

NIH-PA Author Manuscript

NIH-PA Author Manuscript

In conclusion, our in vitro study indicates the presence of a synergistic action between viral (latent infection with JC virus) and environmental (PAH contamination) factors, which dysregulate natural control mechanisms responsible for the maintenance of genomic integrity and uncontrolled DNA replication. Importantly, the abundance of oxidative DNA damage detected in cells and experimental animals chronically exposed to oil-PAHs may suggest the use of antioxidants to counteract this potential carcinogenic action. Finally, JC virus proteins in association with elevated urinary 8-oxo-dG may help in identifying high-risk populations in danger of tumor development in the aftermath of this industrial disaster and future insults.

## Acknowledgments

This work is supported by 2RO1 CA095518 (K.R.) and P20 RR021970 (A.O., K.R.).

## Literature Cited

Abdel-Aziz HO, Murai Y, Hong M, Kutsuna T, Takahashi H, Nomoto K, Murata S, Tsuneyama K, Takano Y. Detection of the JC virus genome in lung cancers: Possible role of the T-antigen in lung oncogenesis. Appl Immunohistochem Mol Morphol. 2007; 15:394–400. [PubMed: 18091381]

Alexander V, Leffingwell SS, Lloyd JW, Waxweiler RJ, Miller RL. Brain cancer in petrochemical workers: A case series report. Am J Ind Med. 1980; 1:115–123. [PubMed: 7342751]

Al-Hashem MA, Brain PF, Omar SA. Effects of oil pollution at Kuwait's greater Al-Burgan oil field on polycyclic aromatic hydrocarbon concentrations in the tissues of the desert lizard Acanthodactylus scutellatus and their ant prey. Ecotoxicology. 2007; 16:551–555. [PubMed: 17879161]

Berger JR, Concha M. Progressive multifocal leukoencephalopathy: The evolution of a disease once considered rare. J Neurovirol. 1995; 1:5–18. [PubMed: 9222338]

Boffetta P, Jourenkova N, Gustavsson P. Cancer risk from occupational and environmental exposure to polycyclic aromatic hydrocarbons. Cancer Causes Control. 1997; 8:444–472. [PubMed: 9498904]

Brodsky JL, Pipas JM. Polyomavirus T antigens: Molecular chaperones for multiprotein complexes. J Virol. 1998; 72:5329–5334. [PubMed: 9620985]

Burczynski ME, Penning TM. Genotoxic polycyclic aromatic hydrocarbon ortho-quinones generated by aldo-keto reductases induce CYP1A1 via nuclear translocation of the aryl hydrocarbon receptor. Cancer Res. 2000; 60:908–915. [PubMed: 10706104]

Carozza SE, Wrensch M, Miike R, Newman B, Olshan AF, Savitz DA, Yost M, Lee M. Occupation and adult gliomas. Am J Epidemiol. 2000; 152:838–846. [PubMed: 11085395]

Collins AR, Oscoz AA, Brunborg G, Gaivao I, Giovannelli L, Kruszewski M, Smith CC, Stetina R. The comet assay: Topical issues. Mutagenesis. 2008; 23:143–151. [PubMed: 18283046]

Curfs DM, Beckers L, Godschalk RW, Gijbels MJ, van Schooten FJ. Modulation of plasma lipid levels affects benzo[a]pyrene-induced DNA damage in tissues of two hyperlipidemic mouse models. Environ Mol Mutagen. 2003; 42:243–249. [PubMed: 14673869]

Del Valle L, Khalili K. Detection of human polyomavirus proteins, T-antigen and agnoprotein, in human tumor tissue arrays. J Med Virol. 2010; 82:806–811. [PubMed: 20336718]

Del Valle L, Gordon J, Assimakopoulou M, Enam S, Geddes JF, Varakis JN, Katsetos CD, Croul S, Khalili K. Detection of JC virus DNA sequences and expression of the viral regulatory protein T-antigen in tumors of the central nervous system. Cancer Res. 2001a; 61:4287–4293. [PubMed: 11358858]

Del Valle, L.; Gordon, J.; Ferrante, P.; Khalili, K. Human polyoviruses molecular and clinical perspectives. 1. New York: Wiley-Liss, Inc; 2001b. JC virus in experimental and clinical brain tumors; p. 409-430.

Del Valle L, Gordon J, Enam S, Delbue S, Croul S, Abraham S, Radhakrishnan S, Assimakopoulou M, Katsetos CD, Khalili K. Expression of human neurotropic polyomavirus JCV late gene product

NIH-PA Author Manuscript

NIH-PA Author Manuscript

NIH-PA Author Manuscript

agnoprotein in human medulloblastoma. J Natl Cancer Inst. 2002a; 94:267–273. [PubMed: 11854388]

Del Valle L, Wang JY, Lassak A, Peruzzi F, Croul S, Khalili K, Reiss K. Insulin-like growth factor I receptor signaling system in JC virus T antigen-induced primitive neuroectodermal tumors-medulloblastomas. J Neurovirol. 2002b; 8:138–147. [PubMed: 12491166]

Demers PA, Vaughan TL, Schommer RR. Occupation, socioeconomic status, and brain tumor mortality: A death certificate-based case-control study. J Occup Med. 1991; 33:1001–1006. [PubMed: 1660541]

Dickey RW. FDA risk assessment of seafood contamination after the BP oil spill. Environ Health Perspect. 2012; 120:a54–a55. [PubMed: 22297092]

Gammon MD, Santella RM. PAH, genetic susceptibility and breast cancer risk: An update from the Long Island Breast Cancer Study Project. Eur J Cancer. 2008; 44:636–640. [PubMed: 18314326]

Goldstein BD, Osofsky HJ, Lichtveld MY. The Gulf oil spill. N Engl J Med. 2011; 364:1334–1348. [PubMed: 21470011]

Hoeijmakers JH. Genome maintenance mechanisms for preventing cancer. Nature. 2001; 411:366–374. [PubMed: 11357144]

Ji G, Gu A, Zhou Y, Shi X, Xia Y, Long Y, Song L, Wang S, Wang X. Interactions between exposure to environmental polycyclic aromatic hydrocarbons and DNA repair gene polymorphisms on bulky DNA adducts in human sperm. PLoS ONE. 2010; 5:1–9.

Jomova K, Valko M. Advances in metal-induced oxidative stress and human disease. Toxicology. 2011; 283:65–87. [PubMed: 21414382]

Kass EM, Jasin M. Collaboration and competition between DNA double-strand break repair pathways. FEBS Lett. 2010; 584:3703–3708. [PubMed: 20691183]

Khalili K, Krynska B, Del Valle L, Katsetos CD, Croul S. Medulloblastomas and the human neurotropic polyomavirus JC virus. Lancet. 1999; 353:1152–1153. [PubMed: 10209983]

Krynska B, Del Valle L, Croul S, Gordon J, Katsetos CD, Carbone M, Giordano A, Khalili K. Detection of human neurotropic JC virus DNA sequence and expression of the viral oncogenic protein in pediatric medulloblastomas. Proc Natl Acad Sci USA. 1999; 96:11519–11524. [PubMed: 10500209]

Krynska B, Del Valle L, Gordon J, Otte J, Croul S, Khalili K. Identification of a novel p53 mutation in JCV-induced mouse medulloblastoma. Virology. 2000; 274:65–74. [PubMed: 10936089]

Liu HH, Lin MH, Chan CI, Chen HL. Oxidative damage in foundry workers occupationally co-exposed to PAHs and metals. Int J Hyg Environ Health. 2010; 213:93–98. [PubMed: 20153695]

Loft S, Poulsen HE, Vistisen K, Knudsen LE. Increased urinary excretion of 8-oxo-2′-deoxyguanosine, a biomarker of oxidative DNA damage, in urban bus drivers. Mutat Res. 1999; 441:11–19. [PubMed: 10224318]

Major EO, Amemiya K, Tornatore CS, Houff SA, Berger JR. Pathogenesis and molecular biology of progressive multifocal leukoencephalopathy, the JC virus-induced demyelinating disease of the human brain. Clin Microbiol Rev. 1992; 5:49–73. [PubMed: 1310438]

Matsiota-Bernard P, De Truchis P, Gray F, Flament-Saillour M, Voyatzakis E, Nauciel C. JC virus detection in the cerebrospinal fluid of AIDS patients with progressive multifocal leucoencephalopathy and monitoring of the antiviral treatment by a PCR method. J Med Microbiol. 1997; 46:256–259. [PubMed: 9126827]

Nakanishi K, Cavallo F, Brunet E, Jasin M. Homologous recombination assay for interstrand cross-link repair. Methods Mol Biol. 2011; 745:283–291. [PubMed: 21660700]

Park JH, Gopishetty S, Szewczuk LM, Troxel AB, Harvey RG, Penning TM. Formation of 8-oxo-7,8-dihydro-2′-deoxyguanosine (8-oxo-dGuo) by PAH o-quinones: Involvement of reactive oxygen species and copper(II)/copper(I) redox cycling. Chem Res Toxicol. 2005; 18:1026–1037. [PubMed: 15962938]

Park JH, Gelhaus S, Vedantam S, Oliva AL, Batra A, Blair IA, Troxel AB, Field J, Penning TM. The pattern of p53 mutations caused by PAH o-quinones is driven by 8-oxo-dGuo formation while the spectrum of mutations is determined by biological selection for dominance. Chem Res Toxicol. 2008; 21:1039–1049. [PubMed: 18489080]

NIH-PA Author Manuscript

NIH-PA Author Manuscript

NIH-PA Author Manuscript

Pierce AJ, Johnson RD, Thompson LH, Jasin M. XRCC3 promotes homology-directed repair of DNA damage in mammalian cells. Genes Dev. 1999; 13:2633–2638. [PubMed: 10541549]

Poulsen HE, Weimann A, Loft S. Methods to detect DNA damage by free radicals: Relation to exercise. Proc Nutr Soc. 1999; 58:1007–1014. [PubMed: 10817169]

Reiss K, Khalili K. Viruses and cancer: Lessons from the human polyomavirus, JCV. Oncogene. 2003; 22:6517–6523. [PubMed: 14528276]

Reiss K, Khalili K, Giordano A, Trojanek J. JC virus large T-antigen and IGF-I signaling system merge to affect DNA repair and genomic integrity. J Cell Physiol. 2006; 206:295–300. [PubMed: 15991250]

Reiss, K.; Khalili, K.; DelValle, L. JC virus association with brain tumors: The role of T-antigen and Insulin-like growth factor I in DNA repair fidelity. In: Khalili, K.; Jeang, K., editors. Viral oncology basic science and clinical applications. Hoboken, NJ: John Wiley & Sons and Blackwell Publishing; 2010.

Reiss K, Del Valle L, Lassak A, Trojanek J. Nuclear IRS-1 and cancer. J Cell Physiol. 2012; 227:2992–3000. [PubMed: 22454254]

Rollison DE, Helzlsouer KJ, Alberg AJ, Hoffman S, Hou J, Daniel R, Shah KV, Major EO. Serum antibodies to JC virus, BK virus, simian virus 40, and the risk of incident adult astrocytic brain tumors. Cancer Epidemiol Biomarkers Prev. 2003; 12:460–463. [PubMed: 12750243]

Rotkin-Ellman M, Wong KK, Solomon GM. Seafood contamination after the BP Gulf oil spill and risks to vulnerable populations: A critique of the FDA risk assessment. Environ Health Perspect. 2012; 120:157–161. [PubMed: 21990339]

Sankpal UT, Pius H, Khan M, Shukoor MI, Maliakal P, Lee CM, Abdelrahim M, Connelly SF, Basha R. Environmental factors in causing human cancers: Emphasis on tumorigenesis. Tumour Biol. 2012; 33:1255–1274. [PubMed: 22430258]

Seike K, Murata M, Oikawa S, Hiraku Y, Hirakawa K, Kawanishi S. Oxidative DNA damage induced by benz[a]anthracene metabolites via redox cycles of quinone and unique non-quinone. Chem Res Toxicol. 2003; 16:1470–1476. [PubMed: 14615974]

Stowers SJ, Anderson MW. Formation and persistence of benzo(a)pyrene metabolite-DNA adducts. Environ Health Perspect. 1985; 62:31–39. [PubMed: 4085435]

Sullivan CS, Tremblay JD, Fewell SW, Lewis JA, Brodsky JL, Pipas JM. Species-specific elements in the large T-antigen J domain are required for cellular transformation and DNA replication by simian virus 40. Mol Cell Biol. 2000; 20:5749–5757. [PubMed: 10891510]

Trojanek J, Ho T, Del Valle L, Nowicki M, Wang JY, Lassak A, Peruzzi F, Khalili K, Skorski T, Reiss K. Role of the insulin-like growth factor I/insulin receptor substrate 1 axis in Rad51 trafficking and DNA repair by homologous recombination. Mol Cell Biol. 2003; 23:7510–7524. [PubMed: 14559999]

Trojanek J, Croul S, Ho T, Wang JY, Darbinyan A, Nowicki M, Del Valle L, Skorski T, Khalili K, Reiss K. T-antigen of the human polyomavirus JC attenuates faithful DNA repair by forcing nuclear interaction between IRS-1 and Rad51. J Cell Physiol. 2006a; 206:35–46. [PubMed: 15965906]

Trojanek J, Ho T, Croul S, Wang JY, Chintapalli J, Koptyra M, Giordano A, Khalili K, Reiss K. IRS-1-Rad51 nuclear interaction sensitizes JCV T-antigen positive medulloblastoma cells to genotoxic treatment. Int J Cancer. 2006b; 119:539–548. [PubMed: 16572421]

Wilk A, Waligorska A, Waligorski P, Ochoa A, Reiss K. Inhibition of ERbeta induces resistance to cisplatin by enhancing Rad51-mediated DNA repair in human medulloblastoma cell lines. PLoS ONE. 2012; 7:e33867. [PubMed: 22439007]

Xue W, Warshawsky D. Metabolic activation of polycyclic and heterocyclic aromatic hydrocarbons and DNA damage: A review. Toxicol Appl Pharmacol. 2005; 206:73–93. [PubMed: 15963346]

NIH-PA Author Manuscript
NIH-PA Author Manuscript
NIH-PA Author Manuscript



**A**

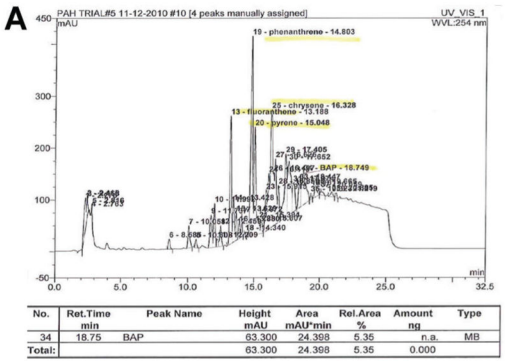


| No. | Ret.Time min | Peak Name | Height mAU | Area mAU*min | Rel.Area % | Amount ng | Type |
|---|---|---|---|---|---|---|---|
| 34 | 18.75 | BAP | 63.300 | 24.398 | 5.35 | n.a. | MB |
| Total: | | | 63.300 | 24.398 | 5.35 | 0.000 | |

**B**

| Extraction date | 11/1/10 | 11/12/10 | 12/17/10 | | | | | |
|---|---|---|---|---|---|---|---|---|
| | ng | ng | ng | Co-eff | Std.Dev. | Slope | Oil-PAHs (μg/ml) | 1/500 (μg/ml) |
| **Benzo {α} pyrene (BaP)** | 305.826 | 404.412 | 501.023 | 98.996 | 10.04 | 0.078 | **8.1 +/- 2** | **0.016** |
| **Fluoranthene (F)** | 1027.057 | 1309.486 | 1673.661 | 99.47 | 5.99 | 0.068 | **26.6 +/- 6.5** | **0.053** |
| **Pyrene (P)** | 450.243 | 449.501 | 777.353 | 97.975 | 14.91 | 0.087 | **11.1 +/- 3.7** | **0.022** |
| **Phenanthanene (Ph)** | 137.552 | 178.289 | 283.964 | 99.97 | 1.66 | 0.277 | **3.9 +/- 1.5** | **0.0078** |
| **Chrysene (C)** | 153.782 | 175.265 | 246.391 | 97.48 | 16.7 | 0.561 | **3.8 +/- 0.98** | **0.0076** |

**C**

| | abs max [nm] | ext max [nm] | em max [nm] |
|---|---|---|---|
| acenaphtylene | | 235 | 315 |
| naphtalene | | 220 | 335 |
| fluorene | | 220 | 317 |
| acenaphtene | | 220 | 340 |
| Phenenthrene | 250 | 252 | 365 |
| Anthracene | | 240 | 395 |
| Fluoranthene | 235 | 235 | 455 |
| Pyrene | 240 | 240 | 390 |
| benzo-a-anthracene | | 235 | 398 |
| Chrysene | 268 | 270 | 380 |
| BaP | 296, 260 | 265 | 410 |
| BgP | 300 | 295 | 420 |
| Coronene | 302 | 304 | 450 |

**Fig. 1.**

High performance liquid chromatography (HPLC) of DMSO extracts from 2010 Deepwater Horizon oil spill in the Gulf of Mexico. Part A: The histogram of DMSO extract of natural crude oil generated by HPLC. The obtained peaks of the oil-PAHs were identified and quantified by comparing their retention times, spectra, and concentrations with a collection of 13 standard PAHs (Part C), which were separated at the same HPLC conditions. Part B: Quantification of the oil-PAHs using three independent DMSO extractions of the same sample of natural crude oil. Each DMSO fraction contained five major peaks, which correspond to the indicated carcinogenic PAHs. Data represent average concentrations ± standard deviation (SD) from three separate extractions in triplicate (n = 9).

NIH-PA Author Manuscript
NIH-PA Author Manuscript
NIH-PA Author Manuscript



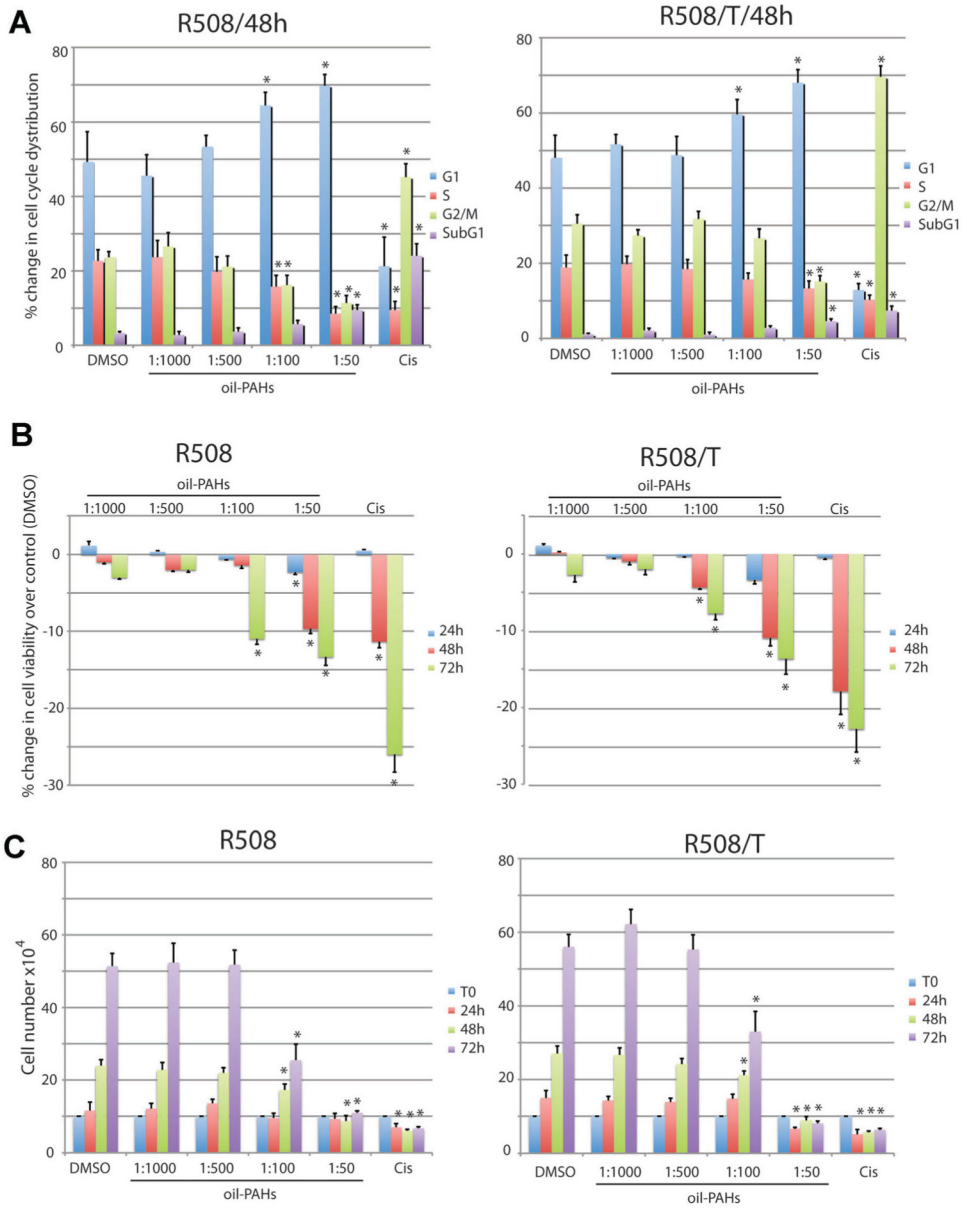


**Fig. 2.**

Evaluation of cytostatic and cytotoxic effects of the oil-PAHs. Evaluation of cell cycle distribution (Part A), cell viability (Part B), and cell number (Part C) during chronic cell exposure to the oil-PAHs. Exponentially growing R508 and R508/T cells (DMEM + 10% FBS) were incubated with different dilutions of the oil-PAHs ranging from 1:50 to 1:1,000. The cells incubated in DMSO (vehicle) were used as negative control and cells incubated with cisplatin (1 μg/ml) were used as positive control for the evaluation of a potential cytostatic and cytotoxic effects of the oil-PAHs. In all parts data represent average values ± SD from at least three independent experiments in triplicates. In part A, *indicates values which are significantly different from the corresponding values of cell cycle distribution (G1, S, G2/M, and sub G1) in cell cultures treated with DMSO. In parts B and C, *indicates values which are statistically different from the values of cell survival (B) and cell number (C) obtained in control conditions (paired Student's *t*-test $P \leq 0.05$).

NIH-PA Author Manuscript
NIH-PA Author Manuscript
NIH-PA Author Manuscript



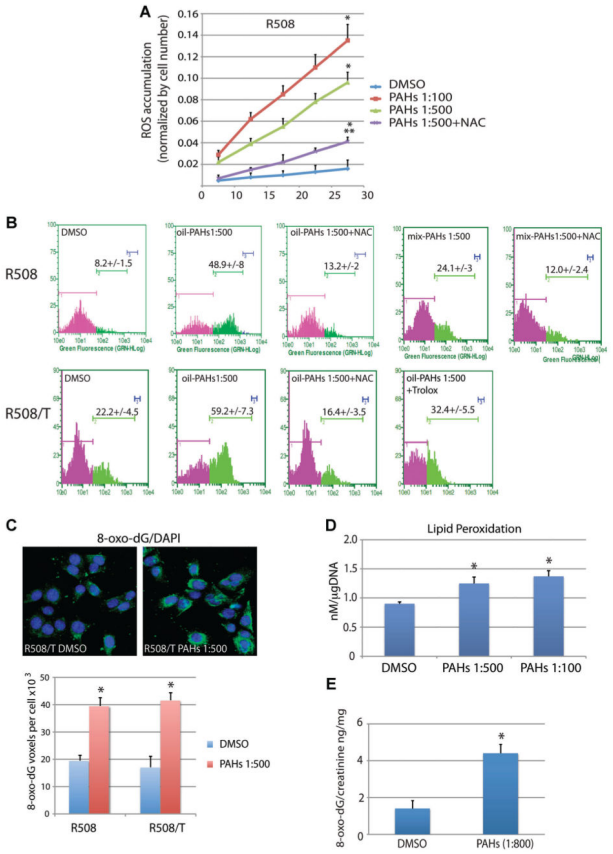


**Fig. 3.**

Detection of ROS and oxidative DNA damage. The accumulation of intracellular ROS was evaluated by two independent techniques: Synergy 2 fluorescent microplate reader (Part A) and flow cytometry (Part B) in cells pre-loaded with 2′,7′-dichlorofluorescin-diacetate (H2DCFDA). R508 and R508/T cells were treated with the oil-PAHs at dilutions 1:100 and 1:500 in the presence or absence of ROS scavengers: *N*-acetylcysteine (NAC; 1 mM) and Trolox (100 μM) for 72 h. The cells treated with DMSO (vehicle) were used as control. Data represent average values ± SD calculated from three independent experiments in duplicates (n = 6). *Indicates ROS accumulation values which are statistically different from the values obtained from DMSO treated samples. **Indicates statistically significant difference from PAHs 1:500 (paired Student's *t*-test $P \leq 0.05$). Part C: Immunocytofluorescent detection of 8-oxo-dG (green fluorescence) in exponentially growing R508 and R508/T cells treated with oil-PAHs (1:500 dilution) for 14 days. Data represent average values ± SD calculated from three independent experiments in duplicate in which at least 50 cells per analysis were evaluated (n = 6). *Indicates values which are statistically different from the value obtained from DMSO (vehicle) treated samples (paired Student's *t*-test $P \leq 0.05$). Part D: Evaluation of lipids peroxidation in cells exposed to oil-PAHs (1:500 and 1:100) for 72 h. Data represent average values ± SD calculated from three independent experiments (n = 3). Part E: Detection of 8-oxo-dG in urine sample from mice fed with the oil-PAHs. The SV129 mice were fed once a day with the vehicle (DMSO diluted with $H_2O$ 1:100) or with the oil-PAH fraction. Data represent average values ± SD calculated from three independent experiments in which three mice per condition were evaluated (n = 9). *Indicates value which is statistically different from the value obtained from DMSO (vehicle) fed mice (paired Student's *t*-test $P \leq 0.05$).

NIH-PA Author Manuscript

NIH-PA Author Manuscript

NIH-PA Author Manuscript

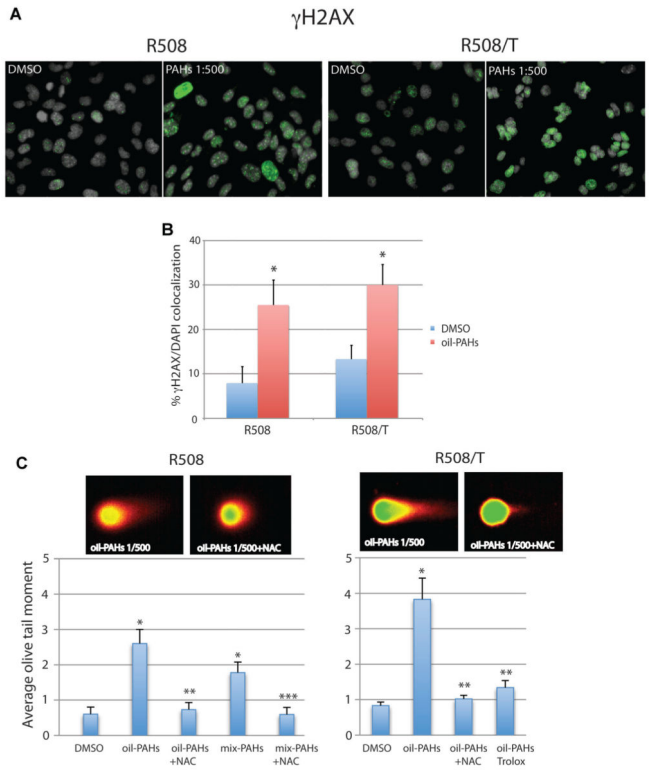


**Fig. 4.**

PAHs-induced γH2AX nuclear foci and DSBs. Part A: Immunofluorescent detection of the phosphorylated form of histone H2AX (γH2AX, green fluorescence) in exponentially growing R508 and R508/T cells treated with oil-PAHs (1:500) for 3 days. Part B: Quantification of nuclear γH2AX foci (DAPI/γH2AX co-localization). Data represent average values ± SD calculated from three independent experiments in triplicate in which at least 100 cells per analysis were evaluated (n = 9). Part C: Neutral comet assay was utilized to detect DNA strand breaks in exponentially growing R508 and R508/T cells, which were exposed to the oil-PAHs (1:500-dilution) in the presence and absence of ROS scavengers NAC (1 mM) and Trolox (100 μM) for 14 days. The cells were subjected to single cell electrophoresis (comet assay) in neutral conditions. Data represent average comet tail moment ± SD calculated from three independent experiments (n = 3); 100 cells per each experimental point were evaluated. *Indicates values which are statistically different from DMSO treated samples. **Indicates values which are significantly different from oil-PAH treated samples. ***Indicates values significantly different from mix-PAHs (paired Student's *t*-test $P \leq 0.05$).

NIH-PA Author Manuscript
NIH-PA Author Manuscript
NIH-PA Author Manuscript



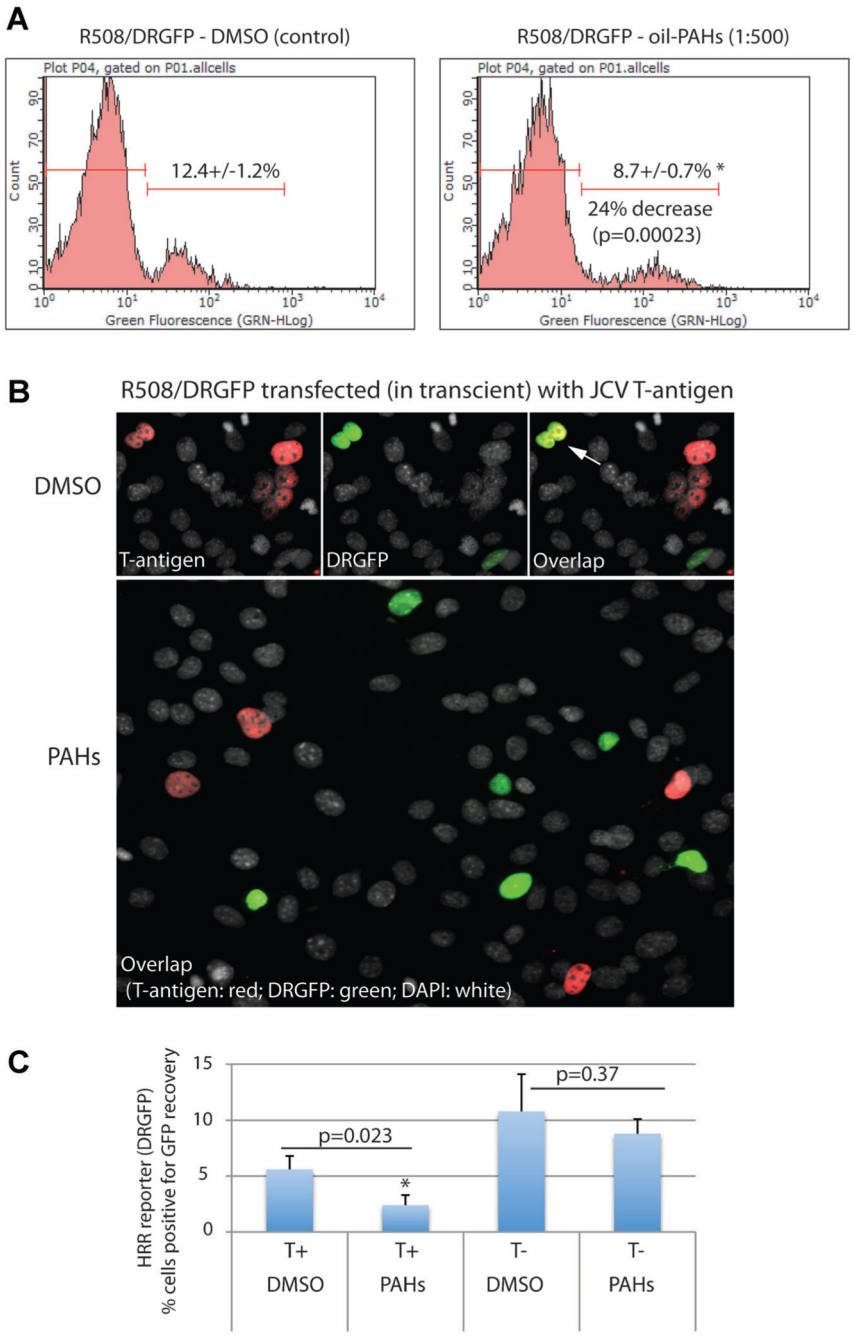


**Fig. 5.**

Effects of oil-PAHs and JCV T-antigen on HRR. Part A: R508 cells expressing HRR reporter plasmid (R508/DRGFP) were transfected in transient with DNA damaging pCβA-Sce expression vector and the cells were cultured in the presence of 10%FBS ± oil-PAHs (1:500) for 96 h. The cells capable of reconstituting GFP function were analyzed by flowcytomentry. The results were collected from three separate experiments, in duplicate (n = 6). Part B: Cytofluorescent detection of HRR in R508/DRGFP cells expressing JCV T-antigen. The cells were transfected (nucleoporation; Amaxa) with pCDNA3/JCV-T/Zeo (Trojanek et al., 2006a) and with pCβA-Sce (Pierce et al., 1999) expression vector. Following 24 h of recovery after transfection, the cells were treated either with oil-PAHs (1:500) or with DMSO (control). JCV T-antigen was detected using

anti-SV40 T-antigen mouse monoclonal antibody (Calbiochem; red fluorescence). DRGFP fluorescence is indicated green, and total nuclei are labeled with DAPI (white fluorescence). Arrow indicates two nuclei in which T-antigen expressing cells are positive for HRR-mediated reconstitution of DR-GFP otherwise the majority of T-antigen expressing cells do not express green. Part C: Quantification of the results depicted in part B. The results were collected from three separate experiments, in duplicate in which 1,000 cells *per* experiment were counted in at least 50 randomly selected microscopic fields. *P*-values are indicated above the compared samples (paired Student's *t*-test $P \leq 0.05$).

NIH-PA Author Manuscript
NIH-PA Author Manuscript
NIH-PA Author Manuscript

NIH-PA Author Manuscript
NIH-PA Author Manuscript
NIH-PA Author Manuscript



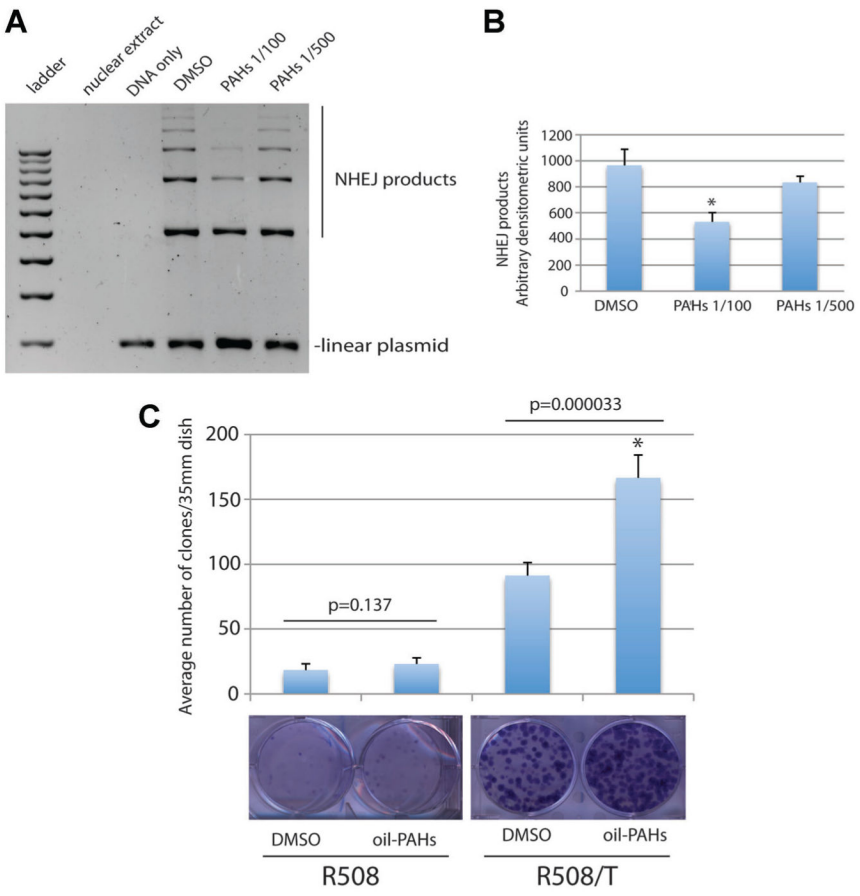


**Fig. 6.**

Effects of oil-PAHs on NHEJ. Part A: NHEJ was evaluated using cell-free assay based on the ability of nuclear extracts to ligate linearized plasmid DNA (Trojanek et al., 2006b). Nuclear extracts were isolated from exponentially growing JCV T-antigen negative (R508) and positive (R508/T) cells, in the presence or absence of the oil-PAHs at 1:100 and 1:500 dilution. Levels of linear plasmid, as well as several multimers formed by NHEJ reaction are indicated. Part B: The histogram illustrating an average of densitometric measurements of NHEJ products obtained from two separate NHEJ experiments. Part C: Clonogenic growth of R508 and R508/T cells exposed to the oil-PAH. Exponentially growing monolayer cultures of R508 and R508/T cells (10% FBS) were either treated with DMSO (control) or with oil-PAHs 1:500 for 4 weeks. The clonogenic growth was evaluated 2 weeks after a continuous cell growth in media containing 10% FBS + DMSO or 10% FBS + oil-PAHs 1:500. Data represent average number of clones ± SD calculated from three independent experiments in duplicate (n = 6). *P* values are indicated above the compared samples (paired Student's *t*-test $P \leq 0.05$).